Relation between shakedown and shape memory of metallic materials considering their mesoscale and atomic scale substructures

V. KAFKA[1)],   D. VOKOUN[2)]

[1)] *Institute of Theoretical and Applied Mechanics, ASCR*
Prosecká 76, 19000 Prague, Czech Republic
e-mail: kafka@itam.cas.cz

[2)] *Institute of Physics, ASCR*
Prosecká 76, 19000 Prague, Czech Republic

SHAKEDOWN (SD) AND SHAPE MEMORY (SM) – generally looked upon as two different phenomena – are shown to have close relations from the point of view of their mechanisms, if considering the respective mesoscale processes on the one hand and the atomic scale processes on the other hand. With the use of the general mesomechanical concept of the first author, their constitutive equations are formulated using the same basic formulae, but with different meanings of the symbols. Constitutive equations are based on the description of internal stresses, in the case of SD on the mesoscale, in the case of SM on the atomic scale. Whereas in the case of SD, plastic deformation means shifting of atomic blocks and changing atomic neighbors, in the case of a diffusionless SM the atomic neighbors are maintained, what simplifies the analysis.

Key words: shakedown, shape memory, mesomechanics, analysis.

Notations

c_p	limit value of s_{11p} at the start of plastic deformation in a uniaxial elastic-plastic process,
$\bar{e}_{ij}, \{e_{ije}, e_{ijp}\}$	macroscopic {mesoscopic} deviatoric strain,
$e'_{ije}, \{e'_{ijp}\}$	deviatoric parts of $\varepsilon'_{ije}, \{\varepsilon'_{ijp}\}$,
E	Young's modulus,
i, j	indices that can take on the values 1, 2, 3; their repetition means summation,
$e\{p\}$	index that relates the respective value to the resistant e-substructure {to the compliant p-substructure}; repetition does not mean summation,
$p = v_e\eta_e + v_p\eta_p$,	
$q = p + \eta_e\eta_p$,	
$\bar{s}_{ij}, \{s_{ije}, s_{ijp}\}$	macroscopic {mesoscopic} deviatoric stress,
$s'_{ije}, \{s'_{ijp}\}$	deviatoric parts of $\sigma'_{ije} \{\sigma'_{ijp}\}$,
v_e	volume fraction of the resistant substructure with only elastic deformation,
$v_p\,(= 1 - v_e)$	volume fraction of the compliant substructure with dissipative deformation,

W_{el} elastic energy of internal stresses comprised in a volume unit of the whole material,

$\bar{\sigma}_{ij}, \{\bar{\varepsilon}_{ij}\}$ macroscopic stress {strain} tensor,

$\varepsilon_{ije}, \{\varepsilon_{ijp}\}$ mesoscopic strain in the resistant {compliant} substructure – averaged values in the respective substructure,

$\sigma_{ije}, \{\sigma_{ijp}\}$ mesoscopic stress in the resistant {compliant} substructure – averaged values in the respective substructure,

δ_{ij} Kronecker's delta,

$\delta_{ij}\bar{\sigma}, \{\delta_{ij}\sigma_e, \delta_{ij}\sigma_p\}$ macroscopic {mesoscopic} isotropic part of the stress tensors,

$\delta_{ij}\bar{\varepsilon}, \{\delta_{ij}\varepsilon_e, \delta_{ij}\varepsilon_p\}$ macroscopic {mesoscopic} isotropic part of the strain tensor,

$\varepsilon'_{ije} = \varepsilon_{ije} - \bar{\varepsilon}_{ij}, \{\varepsilon'_{ijp} = \varepsilon_{ijp} - \bar{\varepsilon}_{ij}\}$ definitions of quantities $\varepsilon'_{ije}, \{\varepsilon'_{ije}\}$,

$\delta_{ij}\varepsilon'_e, \{\delta_{ij}\varepsilon'_p\}$ isotropic parts of $\varepsilon'_{ije}, \{\varepsilon'_{ijp}\}$,

$\sigma'_{ije}, \{\sigma'_{ijp}\}$ stresses related to $\varepsilon'_{ije}, \{\varepsilon'_{ijp}\}$ similarly as are $\sigma_{ije}, \{\sigma_{ijp}\}$ related to $\varepsilon_{ije}, \{\varepsilon_{ijp}\}$,

$\delta_{ij}\sigma'_e, \{\delta_{ij}\sigma'_p\}$ isotropic parts of $\sigma'_{ije}, \{\sigma'_{ijp}\}$,

η_e, η_p structural parameters (non-negative by definition) that characterize the structure of the material [$\eta_e = \eta_p = 0$ corresponds to Voigt's homogeneous strain model, $\eta_e = \eta_p = \infty$ corresponds to Reuss' homogeneous stress model, $0 < \eta_e < \infty$ and $0 < \eta_p < 0$ characterize more general structures; an increase {decrease} of one of the parameters describes a decrease {increase} of connectivity of the respective substructure; a more general explanation is given in the text following Eq. (2.9)],

λ_p scalar measure of plastic deformation in the p-constituent,

Λ_p formal expression whose differential increment $d\Lambda_p$ is defined by Eq. (2.21), in an active dissipative process $d\Lambda_p > 0$ and $d\lambda_p = d\Lambda_p$; otherwise $d\lambda_p = 0$,

$\mu = (1+\nu)/E$ deviatoric elastic compliance,

$\rho = (1-2\nu)/E$ isotropic elastic compliances,

ν Poisson's ratio.

1. Introduction

THE TERM *shakedown* (SD) is used for a *favorable effect of plastic deformations that extend the area of forthcoming cyclic elastic deformations*. On the *macroscale*, in structures, the classical works on SD (e.g. [1–3]) describe this effect of plastic deformations with taking into account a *heterogeneous* redistribution of the *first order* internal stresses, i.e. of macroscopic internal stresses. This redistribution resulting from plastic deformation can lead – after one or more loading cycles – to the sought effect in bodies of different shape and size.

Later a number of papers have been devoted also to the relation between shakedown and shape memory (SM). Thus Wu *et al.* [4] presented a model for the role of repeated stress-temperature cycling on selecting the microstructural variants. Stress-temperature cycling eventually leads to a periodic limit cycle, giving rise to a limiting periodic strain response. FENG and SUN [5] formulated a three-dimensional phenomenological constitutive model for different regimes of elastic-plastic deformation and phase transformation in SM materials. They

found out that the phase transformation might either increase or decrease the load-bearing capacity of a structure. FENG *et al.* [6] introduced the concept of phase transformational shakedown to interpret the wear-resistant behavior of the NiTi shape memory alloy. On the scale of grains, the properties of SM materials have been studied by KOCKAR *et al.* [7]. In their experimental study, they observed the effect of grain size in NiTi alloy. In a material with ultrafine grains they found a notable improvement in the thermal cyclic stability under relatively high stresses.

Our approach attacks the problem with the use of our mesomechanical model published in monograph [8]. It takes into consideration the SD effect in the case of simple uniaxial loading of plastically deforming metallic materials, where the field of the *first order* internal stresses is homogeneous. We use the term *shakedown* in a bit unusual way for the processes in materials instead of structures, but in principle, it models again a *favorable effect of plastic deformations that extends the area of forthcoming cyclic elastic deformations.*

Instead of working with shakedown theorems as it is the case on the macroscale, we base our analysis on our mesomechanical concept. In our approach, a metallic material is described as a heterogeneous medium with two substructures having different forms and mechanical properties. The physical nature of these substructures can be different in different materials. For our way of modeling, it is sufficient to assume that such substructures exist. In metallic materials, the compliant substructure can be attributed to the inner parts of grains with easy glide, the resistant substructure to impurities, precipitates and boundary regions between grains. In the macroscopically observed elastic segments of the stress-strain diagram, the deformation of both the substructures is elastic. This means that all the interatomic bonds remain conservative. In the macroscopically observed inelastic segment, the compliant substructure deforms in an inelastic way, meaning that some of its interatomic distances exceed the limits in which their deformation is conservative, and the deformation starts to be dissipative. In a number of our works, this *mesoscale* model has successfully been applied to metallic materials, concrete and polymers.

The basic formulae of our model have been applied also to the description of shape memory (SM) phenomena [8–12], where the respective variations of interatomic forces and distances have been analyzed in detail. Of course there are substantial differences between applications to SD or to SM. Whereas in the applications to SD the basic formulae are working on the mesoscale, in the applications to SM they are working on the atomic scale. In the current study, we are going to show that in spite of the substantial differences, the principal mechanisms are analogous and therefore, the form of the model can be similar.

In the following sections, the applications of our model to the SD and the SM processes are juxtaposed.

2. The basic model

The basic model used in the current study is a general model for a material with two substructures, deduced in the above-mentioned monograph [8] of the first author. In our previous studies [8, 11, 12], it has been shown that this model can be used also for media with two substructures that have different mechanical properties, but do not have the character of phases. In the applications to SM phenomena, they have the character of two different atomic grids, one of them resistant and remaining elastic, conservative, the other one compliant and deforming in a dissipative way.

The basic set of equations in our model reads:

(2.1) $$v_e \sigma_{ije} + v_p \sigma_{ijp} = \bar{\sigma}_{ij},$$

(2.2) $$v_e \varepsilon_{ije} + v_p \varepsilon_{ijp} = \bar{\varepsilon}_{ij},$$

(2.3) $$\dot{e}_{ije} = \mu \dot{s}_{ije}, \qquad \varepsilon_e = 0,$$

(2.4) $$\dot{e}'_{ije} = \dot{e}_{ije} - \dot{\bar{e}}_{ij}, \qquad \dot{\varepsilon}'_e = 0,$$

(2.5) $$\dot{e}'_{ije} = \mu \dot{s}'_{ije},$$

(2.6) $$\dot{e}_{ijp} = \mu \dot{s}_{ijp} + \dot{\lambda}_p s_{ijp}, \qquad \bar{\varepsilon}_p = 0,$$

(2.7) $$\dot{e}'_{ijp} = \dot{e}_{ijp} - \dot{\bar{e}}_{ij}, \qquad \varepsilon'_p = 0,$$

(2.8) $$\dot{e}'_{ijp} = \mu \dot{s}'_{ijp} - \dot{\lambda}_p s'_{ijp},$$

(2.9) $$\dot{s}_{ije} - \dot{s}_{ijp} + \frac{1}{\eta_e} \dot{s}'_{ije} - \frac{1}{\eta_p} \dot{s}'_{ijp} = 0.$$

For the determination of 9 tensorial variables σ_{ije}, σ_{ijp}, σ'_{ije}, σ'_{ijp}, ε_{ije}, ε_{ijp}, ε'_{ije}, ε'_{ijp}, $\bar{\varepsilon}_{ij}$ there are 9 tensorial equations (2.1) to (2.9) available (if the evolution of $\bar{\sigma}_{ij}$ is prescribed).

The symbols are defined in the Section 'Notations', but it seems that the above set of equations deserves a more detailed explanation:

Equations (2.1) and (2.2) are the commonly used equations for a two-phase composite material. Equations (2.3) and (2.6) are constitutive equations of the two material constituents, written for deviatoric and isotropic parts separately. Symbol $\lambda_p = 0$ represents a scalar measure of plastic deformation in the case of SD analysis, and a scalar measure of the inelastic deformation of the dissipative atomic substructure in the case of SM analysis.

Equations (2.4) and (2.7) define variables e'_{ije} and e'_{ijp} as the differences between average strains in the material constituents and the macroscopic strains. In our model, these variables have been introduced for modeling the effect of

fluctuations (space deviations), as it has been found that working with only average values of stress and strain in the material constituents is not sufficient.

Equations (2.5), (2.8) and (2.9) have been derived in our above-quoted monograph. The derivation of the whole scheme (based among others on the expression for specific stress power formulated on the mesoscale) is not simple and short enough to include it in this short communication, but the following comments try to make the basic features of the model understandable.

The symbols η_e, η_p are called *structural parameters*. They have been derived as integral forms in the distribution functions of stresses and strains in a representative volume element (RVE). In a RVE, the response to a macroscopic stress $\bar{\sigma}_{ij}$ or strain $\bar{\varepsilon}_{ij}$ is described not only by average values of stress and strain in the two substructures of the two material constituents ($\sigma_{ije}, \sigma_{ijp}, \varepsilon_{ije}, \varepsilon_{ijp}$), but also by distribution functions that describe their fluctuations. The distribution functions depend on the configurations of the two substructures, and they are functions of space and time. It was not realizable to work with such complicated distribution functions, and therefore, the model was simplified by assuming that the distribution function can approximately be described as a product of function of space and function of time. Then it was possible – with the use of a variation procedure – to derive their relatively simple characteristics – their integral forms – called *structural parameters*. This variation procedure leads to Eq. (2.9), by which the stress values are bound to the structural parameters, but it gives also substantiation for Eqs. (2.5) and (2.8).

The *distribution functions* and the integral forms, by which the structural parameters have been defined, appeared only in the *derivation* of the model. They do not appear in the final form of the model itself. The user of the model works only with the structural parameters without finding the distribution functions themselves. For the user, the structural parameters are *free parameters* that are to be determined from simple macroscopic experiments – from stress-strain diagrams or flow-curves by their mathematical analysis. The way of their determination is not shown in the current study as it is relatively complicated, and its presentation is not important for the objective of this study. We can only refer the Reader to our above-quoted monograph.

From Eq. (2.9), we see that $\eta_e = \eta_p = \infty \Rightarrow s_{ije} = s_{ijp} = \bar{s}_{ij}$, which means a homogeneous microscopic stress field in the RVE. On the other hand, strains can be different in the two substructures (due to inelastic deformation in the p-substructure), but homogeneous in either substructure. This is Reuss' model.

Similarly, it can be concluded from Eqs. (2.9), (2.4), (2.5), (2.7), (2.8) that $\eta_e = \eta_p = \infty \Rightarrow s'_{ije} = s'_{ijp} = 0 \Rightarrow e_{ije} = e_{ijp} = \bar{e}_{ij}$, which means homogeneous microscopic strain field in the RVE. On the other hand, stresses can be different in these two substructures (due to inelastic strains in the p-constituent), but homogeneous in either material constituent. This is Voigt's model.

For η_e, η_p neither infinite nor vanishing, the corresponding microscopic stress- and strain-fields are not homogeneous in either material constituent. Different finite values of η_e, η_p (non-negative by definition) correspond to different shapes of the two substructures. The integral forms, by which the structural parameters have been defined, imply that the higher is the value of η_e $\{\eta_p\}$, the lower is the connectivity of the e-substructure $\{p$-substructure$\}$. For an infinite value of η_e and a finite value of η_p, the e-substructure forms discontinuous inclusions in the matrix of the p-substructure (and *vice versa*). It is an important feature of our model that with its use, the *degree of connectivity* of the two substructures can easily be characterized.

Based on this concept, the expression for elastic energy comprised in a unit volume RVE of the material reads:

$$(2.10) \quad W_{el} = \frac{1}{2}\left\{\mu\left[v_e\left(s_{ije}s_{ije}+\frac{1}{\eta_e}s'_{ije}s'_{ije}\right)+v_p\left(s_{ijp}s_{ijp}+\frac{1}{\eta_p}s'_{ijp}s'_{ijp}\right)\right]+3\rho\bar{\sigma}^2\right\}.$$

From the above-presented set of Eqs. (2.1)–(2.9), the macroscale constitutive equation can be derived in a straightforward way to give:

$$(2.11) \qquad d\bar{\varepsilon}_{ij} = d\bar{e}_{ij} + \delta_{ij}d\bar{\varepsilon} = \mu d\bar{s}_{ij} + v_p s_{ijp}d\lambda_p + \delta_{ij}\rho d\bar{\sigma},$$

$$(2.12) \qquad ds_{ijp} = d\bar{s}_{ij} - \frac{v_e}{\mu q}(ps_{ijp} - \eta_e s'_{ijp})d\lambda_p,$$

$$(2.13) \qquad ds_{ije} = d\bar{s}_{ij} - \frac{v_p}{\mu q}(ps_{ijp} - \eta_e s'_{ijp})d\lambda_p,$$

$$(2.14) \qquad ds'_{ijp} = \frac{\eta_p}{\mu q}[v_e\eta_e s_{ijp} - (v_p + \eta_e)s'_{ijp}]d\lambda_p,$$

$$(2.15) \qquad ds'_{ije} = \frac{v_p\eta_e}{\mu q}(\eta_p s_{ijp} + s'_{ijp})d\lambda_p,$$

where

$$(2.16) \qquad p = v_e\eta_e + v_p\eta_p, \qquad q = p + \eta_e\eta_p.$$

The newly introduced expressions p and q have no special physical meaning, their formal use only simplifies the equations.

The differential of the scalar measure of plastic deformation $d\lambda_p$ must be determined from a yield criterion. It has been shown in our previous works that the best results – even for complicated loading paths – have been received if the yield criterion was proposed in the form:

$$(2.17) \qquad s_{ijp}s_{ijp} \leq \frac{3}{2}c_p^2 + \frac{1}{\eta_n}s'_{ijp}s'_{ijp}.$$

This is a generalized Mises' criterion, where the second addend on the right-hand side represents the effect of stress fluctuations.

In an active plastic process, the two sides of the criterion are equal, and in a differential form it gives:

$$(2.18) \qquad s_{ijp}ds_{ijp} - \frac{1}{\eta_p}s'_{ijp}ds'_{ijp} = 0.$$

From this equation, the differential $d\lambda_p$ can easily be expressed with the use of Eqs. (2.12) and (2.14):

$$(2.19) \qquad d\lambda_p = 0 \qquad \text{for} \quad s_{ijp}s_{ijp} < \frac{3}{2}c_p^2 + \frac{1}{\eta_p}s'_{ijp}s'_{ijp},$$

$$(2.20) \qquad d\lambda_p = (d\Lambda_p + |d\Lambda_p|)/2 \qquad \text{for} \quad s_{ijp}s_{ijp} = \frac{3}{2}c_p^2 + \frac{1}{\eta_p}s'_{ijp}s'_{ijp},$$

where

$$(2.21) \qquad d\Lambda_p = \mu\frac{qs_{ijp}d\bar{s}_{ijp}}{v_eps_{ijp}s_{ijp} - (v_p + \eta_e)s'_{ijp}s'_{ijp}}.$$

The evolution equations (2.12) to (2.15) of the internal variables are not independent; s_{ije} and s_{ijp} are bound by Eq. (2.1), s'_{ije} and s'_{ijp} by Eq. (2.9). Hence, it is possible to reduce the above presented set of five equations to only three equations, which is shown in what follows.

In our monograph [8], it has been demonstrated that our model leads to a good agreement with experimental data even for very complicated loading paths applied to aluminum alloy and steel samples.

3. Model of material shakedown in the case of uniaxial tension and twisting

Let us apply the general model to uniaxial tension of a metallic bar and torsion of a thin-walled tube. For a tensile loading in the x_1-direction, the constitutive equation (Eqs. (2.11)–(2.15)) can be simplified to:

$$(3.1) \qquad d\bar{\varepsilon}_{11} = d\bar{e}_{11} + d\bar{\varepsilon} = \mu d\bar{s}_{11} + v_p s_{11p}d\lambda_p + \rho d\bar{\sigma},$$

$$(3.2) \qquad ds_{11p} = d\bar{s}_{11} - v_e\frac{ps_{11p} - \eta_es'_{11p}}{\mu q}d\lambda_p,$$

$$(3.3) \qquad ds'_{11p} = \eta_p\frac{v_e\eta_es_{11p} - (v_p + \eta_e)s'_{11p}}{\mu q}d\lambda_p,$$

with only two internal variables s_{11p}, s'_{11p} and their evolution equations.

For a demonstration of the material shakedown, we are going to use the material parameters of an aluminum alloy (Al with Mg) studied in detail in [13] and discussed from other points of view in our monograph. They read:

$$\mu = 2.28 \cdot 10^{-5} \text{ MPa}^{-1}, \qquad \rho = 5.4 \cdot 10^{-6} \text{ MPa}^{-1}, \qquad c_p = 63.66 \text{ MPa},$$

$$v_e = 0.056, \qquad v_p = 0.944, \qquad \eta_e = 2.7433125, \qquad \eta_p = 0.011429242.$$

In the following sections, the effect of different kinds of prestrain on the SD phenomenon is analyzed.

3.1. No prestrain

The stress-strain diagram of this material with no prestrain, subjected to uni-axial tension, is shown in Fig. 1. The diagram was calculated and plotted with the use of the differential equations (3.1), (3.2) and (3.3), where the differentials were replaced by very small finite differences and the plot proceeded step by step. After reaching the elastic limit $(\bar{\sigma}_{11})_{el} \left(= \frac{3}{2} c_p\right)$, the process became elastic-plastic due to plastic deformation of the p-constituent. Up to certain limit values of stress and strain – that can be calculated from the known material parameters – the extent of possible elastic unloading and reloading increases. The limit is marked SD_0, since it can be interpreted as a limit of possible shakedown in the material.
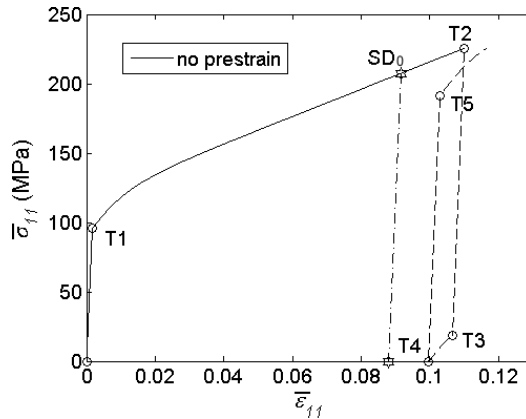

FIG. 1. Stress-strain diagram of the virgin material without any prestrain, with represented limit of elastic unloading SD_0.

For deformation exceeding this limit, unloading is not completely elastic, the end of the unloading segment is elastic-plastic. If the material is looked upon as homogeneous, this fact could seem to contradict the second theorem of thermodynamics, as the macroscopic differential of plastic work in a unit volume RVE is $dW_{pl} = \frac{3}{2} \bar{s}_{11} (d\bar{e}_{11})_{pl}$. This should correspond to the dissipation of energy, but it is negative at the end of unloading. However, if the material is modeled on

the mesoscale, such contradiction does not appear, as the plastic work proceeds only in the p-constituent and is expressed as follows (from Eq. (2.10)):

$$dW_{pl} = \frac{3}{2} v_p \left[(s_{11p})^2 d\lambda_p + \frac{1}{\eta_p} (s'_{11p})^2 d\lambda_p \right],$$

which is unambiguously positive, in loading as well as unloading.

The energy supplied for this plastic work is the energy stored in the material [14–16].

3.2. Tension prestrain

Let us now model the process, in which the body is outstretched in the x_1-direction up to some *plastic prestrain* $(\bar{\varepsilon}_{11})_{ps}$, and then unloaded. Due to this prestrain, there will remain in the material *residual internal stresses* $(s_{11p})_r = -\frac{v_e}{v_p}(s_{11e})_r$, $(s'_{11p})_r$, $(s'_{11e})_r$ that can be calculated with the use of our model. The internal variables, with which our model works, are $(s_{11p})_r$, which is negative, and $(s'_{11p})_r$, which is positive (cf. Table 1).

After this prestrain, a new tension process follows that starts from zero macroscopic stress and strain. It is seen from Fig. 2 that the tensile prestrain causes an *increase* of the elastic limit $(\bar{\sigma}_{11})_{el}$ (point $T4$), and *decrease* of the limit values of stress as well as strain of the point SD (compared with SD_0), where the unloading and reloading is elastic. This phenomenon has practical importance in many cases, where the increase of elastic range is desirable.
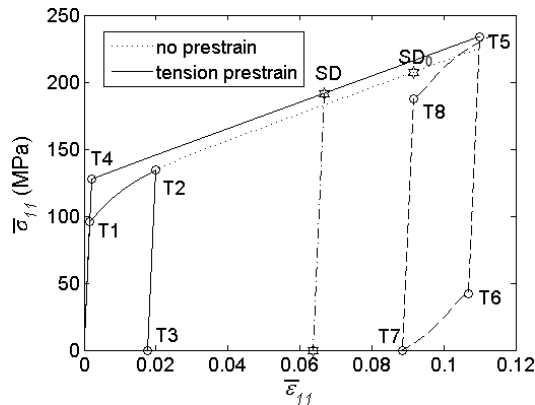

Fig. 2. Stress-strain diagram of the material with tension prestrain.

3.3. Compression prestrain

Furthermore, a similar process is modeled with compressive prestrain. Due to this kind of prestrain, the residual value of $(s_{11p})_r$ will be positive and that of $(s'_{11p})_r$ – negative (cf. Table 1).

The material with these residual internal stresses is then again loaded by tension. The resulting stress-strain diagram is shown in Fig. 3 in comparison with the no-prestrain diagram. It can be seen that the elastic limit $(\bar{\sigma}_{11})_{el}$ (Point $T1$) is lower, the whole diagram is lower, the maximum extent of stress with elastic shakedown is *lower* (SD compared with SD_0), and the limit strain with elastic unloading is *higher*. In some cases, the higher value of the limit strain with elastic unloading and reloading can be of practical importance.
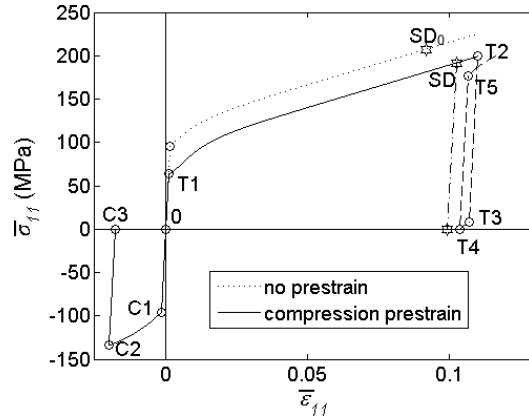

FIG. 3. Stress-strain diagram of the material with compression prestrain.

3.4. Shear prestrain

The third case under consideration is tension of a thin-walled tube that was twisted and unloaded prior to tensile loading. The response to this shear pre-strain $(\bar{\varepsilon}_{12})_{ps}$ (assumed to be positive) and to the subsequent tensile loading is shown in Fig. 4.
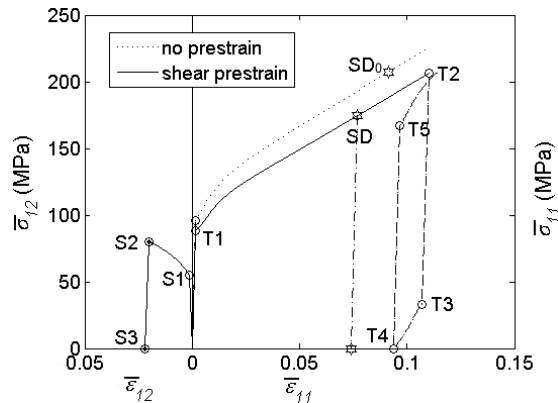

FIG. 4. Stress-strain diagram of the material with shear prestrain.

This time, at the beginning of tensile loading, there are residual internal stresses $(s_{12p})_r = -\frac{v_e}{v_p}(s_{12e})_r$, $(s'_{12p})_r$, $(s'_{12e})_r$. The value of $(s_{12p})_r$ is negative,

the value of $(s'_{12p})_r$ is positive (cf. Table 1). In Fig. 4, the corresponding tensile stress-strain diagram is shown – again in comparison with the no-prestrain diagram. The elastic limit $(\bar{\sigma}_{11})_{el}$ (point $T1$) is *lower*, the whole diagram is lower, the maximum extent of stress with elastic shakedown is *lower* (SD compared with SD_0), and the limit strain with elastic unloading is *lower* (cf. Table 1).

It seems that from the practical point of view the effect of shear prestrain is mostly negative.

Table 1. Characteristic values of stress and strain for different values of prestrain.

	No prestrain	Tension prestrain	Compression prestrain	Shear prestrain
$(\bar{\varepsilon}_{11})_{ps}$ $\{(\bar{\varepsilon}_{12})_{ps}\}$	0	0.02	-0.02	$\{0.02\}$
$(s_{11p})_r$ $\{(s_{12p})_r\}$ (MPa)	0	-21.31	21.31	$\{-20.62\}$
$(s'_{11p})_r$ $\{(s'_{12p})_r\}$ (MPa)	0	2.606	-2.606	$\{2.335\}$
$(\bar{\sigma}_{11})_{el}$ (MPa)	95.5	127.5	63.52	88.54
$(\bar{\varepsilon}_{11})_{SD}$	0.0916	0.0668	0.102	0.0770
$(\bar{\sigma}_{11})_{SD}$ (MPa)	207.4	191.5	191.5	174.5

3.5. Discussion

In the above presented examples, our model is shown to be able to describe the essential character of shakedown in materials. With its use, it is possible to determine the limit of increasing deformation, up to which the unloading and possible reloading and cycling is elastic. This is important information generally, but specifically for the use of overstressing, it is used for improving the resistance of materials to subsequent operational loadings [17].

4. Model of shape memory

In the recently published paper of the first author [11], an overview of applications of our concept to the binary NiTi SM alloy has been presented and discussed. In the current study, we are going to show the relation of these SM applications to material shakedown.

In both cases, the form of the basic set of Eqs. (2.1)–(2.9) is similar, but the meaning of the symbols is different and in the case of SM the processes are temperature-dependent. Whereas in the case of SD the two substructures have the character of phases, in the case of SM of binary alloys the two substructures

have the character of two atomic grids. These two grids differ in their interatomic bonds. In the extent of a one-way SM process, one of the grids remains conservative, i.e. without any energy dissipation of the respective interatomic forces. This *conservative grid* is analogous to the elastic substructure in the model of SD and is represented similarly in the basic equations. The other grid is dissipative, meaning that the distances between the respective atomic pairs extend beyond some limit behind which the elastic energy is dissipated ([8–12]). This *dissipative grid* is analogous to the plastically deforming substructure in the model of SD and is represented similarly.

The *conservative grid* must be strong enough (i) to overpower the resistance of the *dissipative grid*, and (ii) – to preserve the medium in a diffusionless state.

Very often, the models of internal mechanism of SM are based on the description of evolution of dislocations and of internal microstresses, or backstresses [18]. It is common to describe the effect of one dislocation by a microscopic stress field – characterizing the respective field of interatomic forces generated by the dislocation. In the case of a plastic deformation, the shift of atomic blocks makes it impossible to use similarly a microscopic stress field for the representation of a field of dislocations. However, if the deformation process is diffusionless – as it is in the case of the SM processes – such possibility exists, as all the dislocations in a RVE are bound in one closely interactive field. Therefore, in a SM process the changes in the material can be described by internal microstresses, which is the case in our model.

In the case of the *one-way* SM, the dissipative process in the *dissipative grid* is analogous to the plastic dissipative process in the plastically deforming phase in the SD process. Accordingly, the part 0-SD$_0$ of the macroscopically observed stress-strain diagram shown in Fig. 1 is quite similar to what is observed in the loading segment in the *one-way* SM process. The *conservative grid* is not violated in this extent – similarly to the elastic substructure in the case of SD is not violated. After elastic unloading there remain *self-equilibrated residual microstresses* in the two grids. If a stress-free increase of temperature follows after unloading, there proceeds softening of the *dissipative grid* and due to the residual microstresses in the *conservative grid*, the residual macroscopic strain decreases with increasing temperature, and finally it vanishes. In this process the residual microstresses vanish as well.

However, if the originally increasing macroscopic deformation exceeds some limit, the interatomic distances between the atomic pairs in some parts of the *conservative grid* extend beyond a certain limit behind which the elastic energy is dissipated (similarly as in the dissipative grid). This means a violation of the basic conservative character of this grid and due to it, the unloading is not fully elastic. After unloading, an increase of temperature causes again softening of the *dissipative grid*, but the preceding violation of the *conservative*

grid causes that the residual macroscopic deformation is reduced only partly, it does not vanish completely. Accordingly, neither the residual microstresses vanish completely. There remain some microstresses even after the heating. These remaining microstresses represent the basis for the *two-way* SM. A number of different methods called *training* have been proposed [19–21] seeking the best way of creation this remaining microstress state. In the case when unloading and heating is followed by a decrease of temperature, the interatomic distances in the *conservative grid* are shortened, which leads to 'healing' of this grid, to its backward strengthening, and to an increase of macroscopic strain. If this is followed by a new heating, it leads to a decrease of macroscopic strain analogously to the *one-way* process. Thus, cycles of increase and decrease of temperature lead to cycles of decrease and increase of the macroscopic strain, which is called the *two-way* SM (for details see [11]).

5. Conclusion

The general model of the first author [8], originally called and used as *mesomechanical*, can be used for the description of the material SD processes as well as of the SM processes.

If used for the description of the SD processes, the model works on the mesoscale.

If used for the description of the SM processes, the model works on the atomic scale, where the interatomic forces and the changes of interatomic distances in two atomic grids are described and handled as microstresses and microstrains, respectively.

Hence, the background of both these phenomena consists in an interaction of two substructures; their physical nature is different, but the essential mechanical processes are analogous.

Acknowledgment

References

1. E. MELAN, *Zur Plastizität des räumlichen Kontinuums*, Ing. Arch., **9**, 115–126, 1938.

2. W.T. KOITER, *A new general theorem on shakedown of elastic-plastic structures*, Proc. Konink. Nederl. Akad. Wetensch, **B 59**, 24–34, 1956.

3. J.A. KÖNIG, *Shakedown of elastic-plastic structures*, Elsevier, Amsterdam 1987.

4. X. Wu, D.S. Grummon, T.J. Pence, *Modeling phase fraction shakedown during thermomechanical cycling of shape memory materials,* Materials Science and Engineering, A, **273–275**, 245–250, 1999.

5. X.Q. Feng, Q. Sun, *Shakedown analysis of shape memory alloy structures*, International Journal of Plasticity, **23**, 183–206. 2007.

6. X.Q. Feng, L. Qian, W. Yan, Q. Sun, *Wearless scratch on NiTi shape memory alloy due to phase transformational shakedown*, Appl. Phys. Lett., **92**, 121909, 2008.

7. B. Kockar, I. Karaman, J.I. Kim, Y.I. Chumlyakov, J. Sharp, C.J. Yu, *Thermomechanical cyclic response of an ultrafine-grained NiTi shape memory alloy*, Acta Materialia, **56**, 3630–3646, 2008.

8. V. Kafka, *Mesomechanical Constitutive Modeling*, World Scientific, Singapore 2001.

9. V. Kafka, *Shape memory: A new concept of explanation and of mathematical modeling, Part I: Micromechanical explanation of the causality in the SM processes*, J. Intel. Mat. Syst. and Structures, **5**, 809–814, 1994.

10. V. Kafka, *Shape memory: A new concept of explanation and of mathematical modeling, Part II: Mathematical modelling of the SM effect and pseudoelasticity*, J. Intel. Mat. Syst. and Structures, **5**, 815–824, 1994.

11. V. Kafka, *An overview of applications of the mesomechanical approach to shape memory phenomena – completed by a new application to two-way shape memory,* J. Intel. Mat. Syst. and Structures, **19**, 3–17, 2008.

12. V. Kafka, and D. Vokoun, *Background of two characteristic features of shape memory phenomena*, J. Intel. Mat. Syst. and Structures, **17**, 511–520, 2006

13. T. Inoue, K. Yamamoto, *Static and cyclic deformations of quasihomogeneous elastic-plastic material*, Proc. XXIII Japan Congress on Material Research, The Society of Material Science, Kyoto 1980, 12–17.

14. V. Kafka, *Zur Thermodynamik der plastischen Verformung*, ZAMM, **54,** 649–657, 1974.

15. V. Kafka, *Strain-hardening and stored energy*, Acta Technica ČSAV, **24**, 199–216, 1979.

16. V. Kafka, *On some apparent paradoxes in mechanics of deformation and damage of materials* [in Czech], Inženýrská Mechanika, **1**, 177–183, 1994.

17. R.W. Nichols, *The use of overstressing techniques to reduce the risk of subsequent brittle fracture*, British Welding Journal, **15**, 21–42, 75–84, 1968.

18. K. Wada, Y. Liu, *On the two-way shape memory behavior in NiTi alloy – An experimental analysis*, Acta Materialia, **56**, 3266–3277, 2008.

19. J.M.G. Fuentes, P. Gümpel, J. Strittmatter, *Phase change behavior of nitinol shape memory alloys*, Advanced Engineering Materials, **4**, 437–451, 2002.

20. Z.G. Wang, X.T. Zu, X.D. Feng, J.Y. Dai, *Effect of thermomechanical treatment on the two-way shape memory effect of NiTi alloy spring*, Materials Letters, **54**, 55–61, 2002.

21. D.A. Miller, D.C. Lagoudas, *Influence of cold work and heat treatment on the shape memory effect and plastic strain development of NiTi*, Mater. Sci. Eng., A, **308**, 161–175, 2001.